이학석사 학위논문

An ICE-Mediated Transcriptional Feedback Loop Underlies the Transient Induction of Cold-Responsive Genes during Cold Acclimation in *Arabidopsis*

애기장대의 저온순화과정시 ICE 전사인자의 feedback loop을 통한 저온 반응성 유전자의 일시적인 발현 양상 조절에 관한 연구

2014 년 8 월

서울대학교 대학원

화학부 생화학전공

김 예 슬

ABSTRACT

An ICE-Mediated Transcriptional Feedback Loop Underlies the Transient Induction of Cold-Responsive Genes during Cold Acclimation in *Arabidopsis*

Kim Ye Seul

Biochemisty, Department of Chemistry

The Graduate School

Seoul National University

During cold acclimation, C-repeat binding factors (CBFs) activate an array of downstream targets, such as *cold-regulated* (*COR*) genes, leading to the acquisition of freezing tolerance in plants. Inducer of CBF expression 1 (ICE1) plays a key role by activating *CBF3* expression in shaping the cold-induced transcriptome. While the ICE1-CBF3 regulon constitutes a major cold acclimation pathway, gene regulatory networks governing the CBF signaling are poorly understood. Here, we demonstrated that ICE1 and its paralog ICE2 induce *CBF1*, *CBF2*, and *CBF3* by binding to MYC-recognition elements in the gene promoters. ICE2, like ICE1, was ubiquitinated by the high expression of osmotically responsive gene 1 (HOS1) E3 ubiquitin

ligase. Whereas *ICE2*-defective *ice2-2* mutant did not exhibit any discernible freezing-sensitive phenotypes, *ice1-2 ice2-2/+* plant, which is defective in *ICE1* and has a heterozygotic *ice2* mutation, exhibited significantly reduced freezing tolerance. Accordingly, all three *CBF* genes were markedly down-regulated in the *ice1-2 ice2-2/+* plant, indicating that ICE1 and ICE2 are functionally redundant with different implementations in inducing *CBF* genes. On the basis of the negative regulation of *CBF1* and *CBF3* by CBF2 and our own data, we propose that the unified ICE-CBF pathway provides a transcriptional feedback of freezing tolerance to sustain plant development and survival during cold acclimation.

Keywords: ICE, CBF, Cold acclimation, Feedback loop, Unequal redundancy, *Arabidopsis*

Student number: 2012-20270

CONTENTS

INTRODUCTION

Low temperature is a major environmental constraint that limits survival, productivity, and ecological distribution of plants. Plants have evolved diverse adaptation mechanisms to induce freezing tolerance in response to low but non-freezing temperatures, which is referred to as cold acclimation (Chinnusamy et al., 2007). Low temperature influences an extensive set of genes, reshaping the transcriptome (Matsui et al. 2008; Zeller et al. 2009). The low temperature-induced alterations in gene expression provoke a wide array of physiological and biochemical adjustments, such as changes in lipid composition of cellular membranes and accumulation of compatible solutes, cryoprotective compounds, and antifreeze proteins (Guy et al., 2008; Medina et al., 2011).

C-repeat binding factors (CBFs) are APETALLA2 (AP2)-type transcriptional activators and constitute a central component of cold signaling networks that elicit freezing tolerance (Gilmour et al., 1998). Cold-activated CBFs bind to C-repeat (CRT)/dehydration-responsive (DRE) elements in the promoters of downstream targets, such as *cold-regulated* (*COR*) genes (Sakuma et al., 2002; Akhtar et al., 2012). Transgenic *Arabidopsis* plants overexpressing *CBF* genes exhibit enhanced freezing tolerance, which is accompanied by the induction of *COR* genes (Gilmour et al., 2000,

2004). Meanwhile, it has been reported that freezing tolerance is enhanced in *CBF2*-deficient mutants, in which *CBF1* and *CBF3* are up-regulated (Novillo et al., 2004), indicating that CBF2 negatively regulate *CBF1* and *CBF3*. In addition, whereas CBF1 and CBF3 activate a set of cold-responsive genes, CBF2 negatively regulates the same set of genes (Novillo et al., 2007), suggesting that CBF2 is functionally distinct from CBF1 and CBF3 in inducing freezing tolerance. It is likely that coordinated actions of CBFs are required for cold acclimation.

The CBF signaling pathway is regulated by a MYC-like basic helix-loop-helix (bHLH) transcription factor, inducer of CBF expression 1 (ICE1). ICE1 activates *CBF3* by binding to MYC-recognition sequences in the gene promoter (Chinnusamy et al., 2003). It has been reported that the dominant negative *ice1-1* mutant exhibits reduced freezing tolerance, and *CBF3* expression is reduced in the mutant, while *CBF1* and *CBF2* are largely uninfluenced (Chinnusamy et al., 2003). Although *CBF1* and *CBF2* promoters harbor MYC-recognition sequences (Doherty et al., 2009; Lee and Thomashow, 2012), it is unknown whether ICE1 directly regulates their expression.

ICE1 activity is regulated primarily at the protein level (Chinnusamy et al., 2003; Miura et al., 2007). It has been known that low temperature-induced sumoylation of ICE1 by the SIZ1 SUMO E3 ligase is important for the stabilization and activation of

ICE1 (Miura et al., 2007). On the other hand, the high expression of osmotically responsive gene 1 (HOS1) E3 ubiquitin ligase directs the degradation of ICE1 through the ubiquitin/proteasome pathway and thus acts as a cold signaling attenuator (Dong et al., 2006). It has been suggested that HOS1-mediated ICE1 degradation is responsible at least in part for the transient nature of *CBF* induction during cold acclimation (Dong et al., 2006).

It is notable that ICE1/SCRM and its paralog ICE2/SCRM2 also constitute a core regulatory element of stomatal development. The gain-of-function *scrm-D*/*ice1-1* mutant exhibits constitutive stomatal formation in the epidermis of the leaves (Kanaoka et al., 2008). ICE1 and ICE2 are functionally redundant in regulating the stomatal development by forming dimers with a set of bHLH transcription factors that mediates sequential differentiation events during the developmental process. The dual roles of ICE1 in freezing tolerance and stomatal development suggest that ICE1, and perhaps ICE2 as well, serves as a molecular knob that links environmental adaption with plant development (Hofmann, 2008).

ICE1 and ICE2 have a sequence identity of ~60% throughout the full amino acid sequences with essentially identical residues in the DNA-binding bHLH domains (Fursova et al., 2009). Overexpression of *ICE2* leads to dramatic increase of cold-

responsive *CBF1* expression and improved freezing tolerance, suggesting that ICE2 positively regulates *CBF* genes (Fursova et al., 2009). However, it has not been explored how ICE2 regulates *CBF* genes. In addition, the functional relationship between ICE1 and ICE2 has not been investigated in inducing freezing tolerance.

Here, we report a unified ICE-CBF cold acclimation pathway that involves two ICE members and three CBF proteins, in which ICE1 and ICE2 are functionally redundant with different implementations in inducing *CBF* genes. Both ICE1 and ICE2 induce *CBF2*, whose gene product negatively regulates *CBF1* and *CBF3* (Novillo et al., 2004), as well as *CBF1* and *CBF3* by binding directly to MYC-recognition sequences in the gene promoters. It is thus evident that the ICE-CBF2-CBF1/CBF3 signaling module constitutes a transcriptional feedback loop that attenuates cold signaling. We propose that the coordinated regulation of *CBF* genes by ICE1 and ICE2 through the transcriptional feedback loop underlies the expression peak of cold response genes in the early stage of cold acclimation and would be required for persistent plant development during a prolonged exposure to low temperature.

RESULTS

Growth Phenotypes of *ICE*-Defective Mutants

With an aim of elucidating the functional relationship between ICE1 and ICE2 in cold acclimation, we obtained *Arabidopsis* mutants that are defective in either *ICE1* or *ICE2*. In addition to T-DNA insertional *ice1-2* mutant (Kanaoka et al., 2008), we isolated an allele of *ICE2* gene (*ice2-2*) carrying a T-DNA insertion in the second intron (Figure 1A). Gene expression analysis showed that *ice2-2* is a loss-of-function mutant.

Seedlings of *ice1-2* and *ice2-2* mutants were not phenotypically different from Col-0 seedlings except for the slightly shorter petioles in *ice1-2* seedlings (Figures 1B and 1C). Fully grown mutants also showed no discernable phenotypic changes (Figure 1D). In contrast, seedlings of homozygotic *ice1-2 ice2-2* double mutant were severely dwarfed and eventually died at the early growth stages (Figure 1B), as has been reported previously (Zhu et al., 2011), indicating that inactivation of both *ICE1* and *ICE2* is lethal to plant development.

Because of the lethality of homozygotic double mutant, we examined growth phenotypes of *ice1-2/+ ice2-2* and *ice1-2 ice2-2/+* plants that are heterozygotic in *ice1* and *ice2* mutations, respectively. The *ice1-2/+ ice2-2* plants are phenotypically indistinguishable from

Col-0 plants and single mutants (Figures 1B and 1C). Notably, the *ice1-2 ice2-2/+* plants exhibited severely dwarfed growth with shorter petioles. Despite the dwarfed growth, they survived and produced flowering (Figure 1D). These observations indicate that ICE1 and ICE2 have overlapping functions in plant development and ICE1 predominates in the overall ICE function.

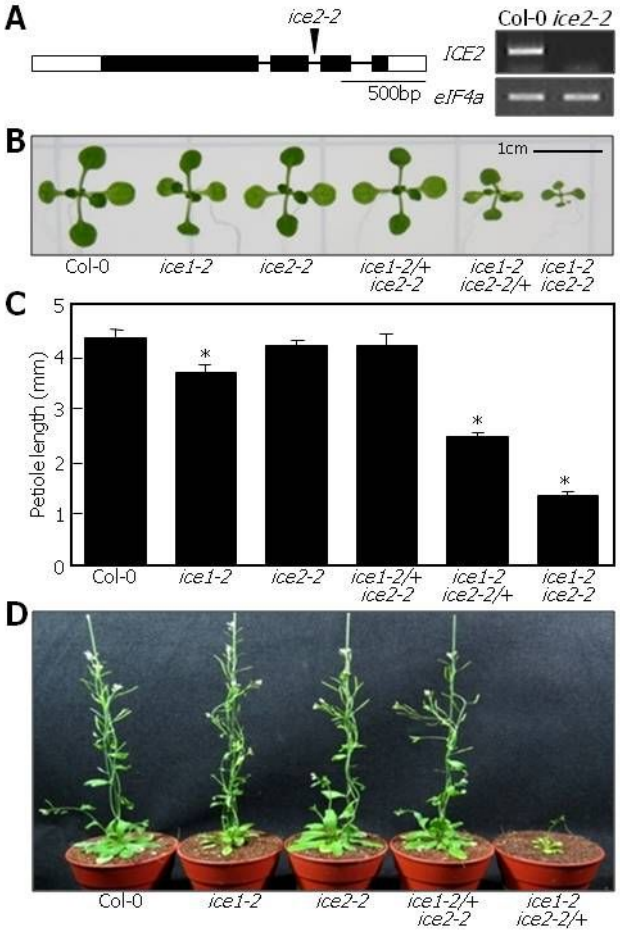

Figure 1. Growth Phenotypes of *ICE*-Defective Mutants.

The *ice1-2* and *ice2-2* mutants were crossed to produce *ice1-2 ice2-2* double mutant. Both homozygotic and heterozygotic plants (*ice1-2 ice2-2* and *ice1-2 ice2-2*/+, respectively) were included in the assays.

(A) Mapping of T-DNA insertion sites in *ice2-2* mutant. Arrowheads indicate the sites of T-DNA insertion (left panel). Black and white boxes represent exons and untranslated regions,

respectively. bp, base pair. The *ice2-2* mutant (GABI-Kat-175D04) was isolated from the *Arabidopsis* mutant pool of T-DNA insertion lines deposited in the German Plant Genomics Research Program-Kölner *Arabidopsis* T-DNA lines (GABI-Kat; Kleinboelting et al., 2012). Lack of *ICE2* expression in the *ice2-2* mutant was verified by RT-PCR (right panel). *eIF4a* gene was included in the assay as control for constitutive expression.

(B) Growth phenotypes of seedlings. Seedlings were grown on MS-agar plates for 12 d at 23^{o}C under LDs.

(C) Measurements of petiole length. The petiole lengths of 12-day-old seedlings shown in (**A**) were measured. Measurements of 20 seedlings were averaged for each plant genotype and statistically treated using Student *t*-test (*P<0.01). Bars indicate standard error of the mean (SE).

(D) Growth phenotypes of fully grown plants. Plants were grown in soil for 40 d under LDs.

ICE1 and ICE2 Are Functionally Redundant in Freezing Tolerance

Considering the role of ICE1 in freezing tolerance, high sequence identity between ICE1 and ICE2, and overlapping roles of ICE1 and ICE2 in stomatal development, we anticipated that ICE2 might also play a role in freezing tolerance.

When plants were exposed to low temperatures (-3°C to -6°C) without cold acclimation, *ice1-2* and *ice2-2* single mutants and *ice1-2 ice2-2*/+ plants did not exhibit any discernible changes in freezing tolerance (Figure 2A), as examined by survival test (Figure 2B) and electrolyte leakage assay (Figure 2C). These observations indicate that ICE1 and ICE2 are not involved in basal resistance to low temperature.

We next performed freezing tolerance assays on cold-acclimated plants. The *ice1-2* mutant exhibited reduced freezing tolerance by approximately 30% at -7°C or lower temperatures under our assay conditions (Figures 2D, 2E, and 2F). The low temperature responses of the *ice1-2* mutant were rescued when *ICE1* gene was expressed driven by the endogenous promoter in the mutant (Figure 3), illustrating that the freezing-sensitive phenotype of the *ice1-2* mutant is caused by the loss of ICE1 function. On the other hand, *ice2-2* mutant did not show any freezing-sensitive phenotype (Figures 2D, 2E, and 2F), obscuring the role of

ICE2 in freezing tolerance.

Notably, cold-acclimated *ice1-2 ice2-2/+* plants were severely sensitive to low temperature (Figures 2D, 2E, and 2F). Whereas *ice1-2* mutant was resistant to -6°C, *ice1-2 ice2-2/+* plants showed a survival rate of 55% at the same temperature (Figure 2E). In addition, the *ice1-2 ice2-2/+* plants exhibited more severe sensitivity than the *ice1-2* mutant at -7°C or lower temperatures in both survival tests and electrolyte leakage assays (Figures 2E and 2F). These observations indicate that the reduced freezing tolerance of the *ice1-2 ice2-2/+* plants is not caused by neither impaired constitutive freezing tolerance nor dwarfed growth but by the reduced capacity of cold acclimation. It is also evident that ICE1 and ICE2 play overlapping roles with unequal functional redundancy in acquiring freezing tolerance.

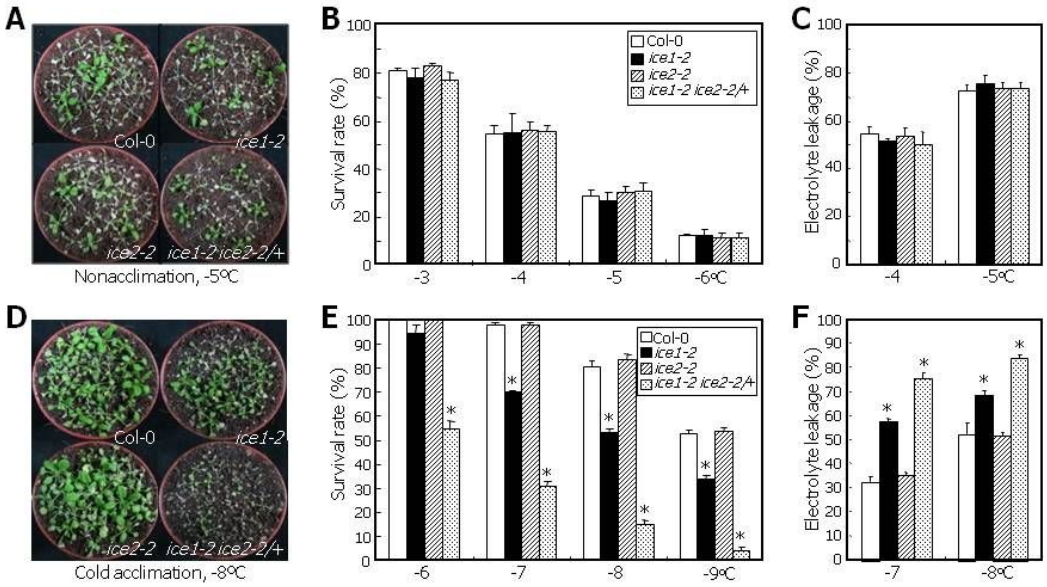

Figure 2. ICE1 and ICE2 Are Functionally Redundant in Inducing Freezing Tolerance.

(A to C) Freezing tolerance of non-acclimated plants. Twelve-day-old plants grown on MS-agar plates were transferred to soil and grown for 3 additional days. They were exposed to freezing temperatures for 3 h. After incubation at 4°C overnight for thawing, they were allowed to recover by incubating at 23°C for 7 d. Plants exposed to -5°C were photographed **(A)**. Survival rates were calculated using 25-30 plants for each plant genotype, and three measurements were averaged and statistically treated using Student *t*-test (**P*<0.01) **(B)**. Electrolyte leakage assays were also employed to examine freezing tolerance **(C)**. Three measurements were averaged and statistically treated using Student *t*-test (**P*<0.01). Bars indicate SE.

(D to F) Freezing tolerance of cold-acclimated plants. Twelve-day-old plant grown on MS-agar

plates were transferred to soil and grown for 3 additional days. They were cold-acclimated by incubating at 4^{o}C for 4 d. Exposure to freezing temperatures, survival test, and electrolyte leakage assay were performed as described in **(A-C)**.

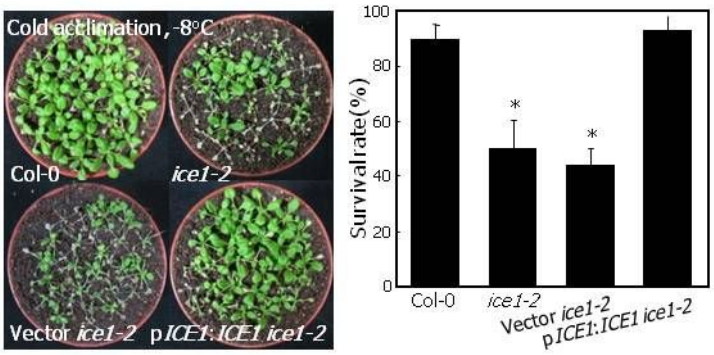

Figure 3. Complementation of *ice1-2* Mutant with Wild-Type *ICE1* Gene.

Wild-type *ICE1* gene was expressed driven by the endogenous *ICE1* promoter consisting of approximately 4-kbp sequence upstream of the translational start site in the *ice1-2* mutant. Freezing treatment (left panel) and calculation of survival rate (right panel) were performed as described in **Figure 2**. Bars indicate SE (*t*-test, **P*<0.01).

CBF Genes Are Suppressed in *ice1-2 ice2-2/+* Plants

It has been reported that only *CBF3* is affected by *ice1* mutations (Chinnusamy et al., 2003). We found that *ice1-2 ice2-2/+* plants are more susceptible to freezing temperatures than *ice1-2* mutant. We therefore examined the expression of *CBF1*, *CBF2*, and *CBF3* in the *ice1-2 ice2-2/+* plants by quantitative real-time RT-PCR (qRT-PCR).

Exposure to cold temperature (4^{o}C) significantly induced the *CBF* genes and their downstream targets, such as *COR15a*, *COR47*, *responsive to desiccation 29A* (*RD29A*), and *kinase 1* (*KIN1*) (Figure 4). In *ice1-2* mutant, the inductive effects of cold temperature on *CBF3* were reduced, while those on other *CBFs* and downstream targets were not largely influenced (Figure 4). In contrast, *ICE2* mutation did not affect any of the *CBF* genes and downstream targets (Figure 4), consistent with the lack of any changes in low temperature responses in the *ICE2*-defective mutant.

It was interesting that *CBF1* and *CBF2* as well as *CBF3* were down-regulated and *CBF3* suppression was more prominent in *ice1-2 ice2-2/+* plants than in *ice1-2* mutant (Figure 4). All the tested downstream targets were also influenced more severely in the *ice1-2 ice2-2/+* plants. These observations support the functional redundancy between ICE1 and ICE2 in cold acclimation.

MYB15 is a negative regulator of *CBF* expression, and ICE1 suppresses *MYB15* gene (Agarwal et al., 2006). We found that *MYB15* gene was slightly induced in *ice1-2* mutant and the inductive effects were significantly elevated in *ice1-2 ice2-2*/+ plants (Figure 4), further supporting the overlapping roles of ICE1 and ICE2 in cold acclimation.

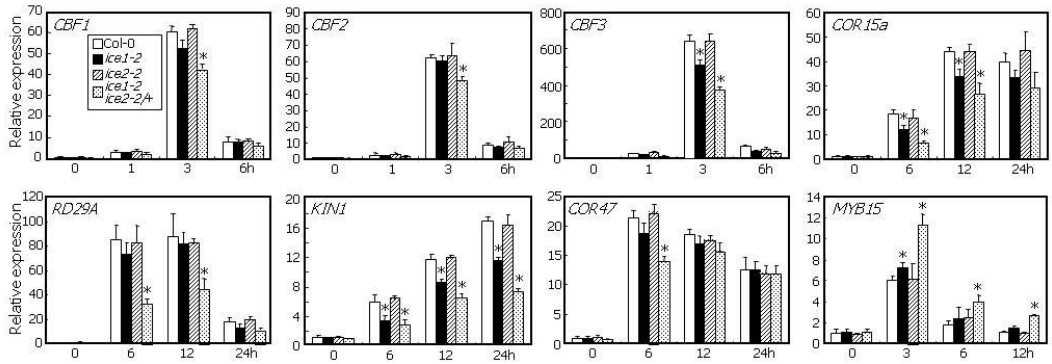

Figure 4. Cold Induction of *CBF* and its Downstream Genes in *ice1-2 ice2-2*/+ Plants.

Two-week-old plants grown on MS-agar plates were exposed to 4°C for the indicated time periods. Whole plants were used for total RNA extraction. mRNA levels were examined by qRT-PCR. Biological triplicates were averaged and statistically treated using Student *t*-test (*P<0.01). Bars indicate SE.

ICE1 and ICE2 Bind to *CBF* Promoters

ICE1 is a transcriptional activator of *CBF3* (Chinnusamy et al., 2003). The suppression of all *CBF* genes in *ice1-2 ice2-2/+* plants suggested that ICE1 and ICE2 regulate the *CBF* genes, possibly by binding directly to the gene promoters.

We first examined whether ICE2 has a transcriptional activation activity by GAL4 transient expression assays in *Arabidopsis* protoplasts. In the effector constructs, *ICE2* sequence was fused in-frame to the GAL4 DNA binding domain-coding sequence (Figure 5A). *ICE1* gene was included as positive control in the assays. *Arabidopsis* protoplasts, in which the ICE2 effector construct and the β-glucuronidase (GUS) reporter construct were coexpressed, exhibited elevated GUS activity (Figure 5B), showing that ICE2 is a transcriptional activator.

We next investigated whether ICE1 and ICE2 bind directly to *CBF1*, *CBF2*, and *CBF3* promoters by chromatin immunoprecipitation (ChIP) assays. It has been proven that approximately 1.2-kb sequence regions upstream of the translational start sites are sufficient for the low temperature induction of the *CBF* genes (Novillo et al., 2007). Sequence analysis identified several potential MYC-recognition sequences in the *CBF* promoters (Figure 5C), to which bHLH transcription factors bind (Meshi and Iwabuchi, 1995). ChIP assays using 35S:*MYC-ICE1* and 35S:*MYC-ICE2* transgenic plants, in which a MYC-coding sequence was

fused in-frame to the 5' ends of *ICE1* and *ICE2*, respectively, revealed that both ICE1 and ICE2 bound to the MYC-recognition sequences in the *CBF* promoters (Figure 5D). Together with the suppression of *CBF* genes in *ice1-2 ice2-2/+* plants, these observations indicate that ICE1 and ICE2 regulate the expression of *CBF1*, *CBF2*, and *CBF3* by binding directly to the gene promoters.

It was anticipated that ICE2 binding to the gene promoters might affect the DNA binding of ICE1. To examine the hypothesis, ChIP assays were performed using *ice2-2* mutant overexpressing the *MYC-ICE1* fusion driven by the Cauliflower Mosaic Virus (CaMV) 35S promoter (35S:*MYC-ICE1 ice2-2*). It was found that ICE2 does not discernibly affect the binding of ICE1 to DNA (Figure 5E), showing that DNA binding events of ICE1 and ICE2 are independent of each other.

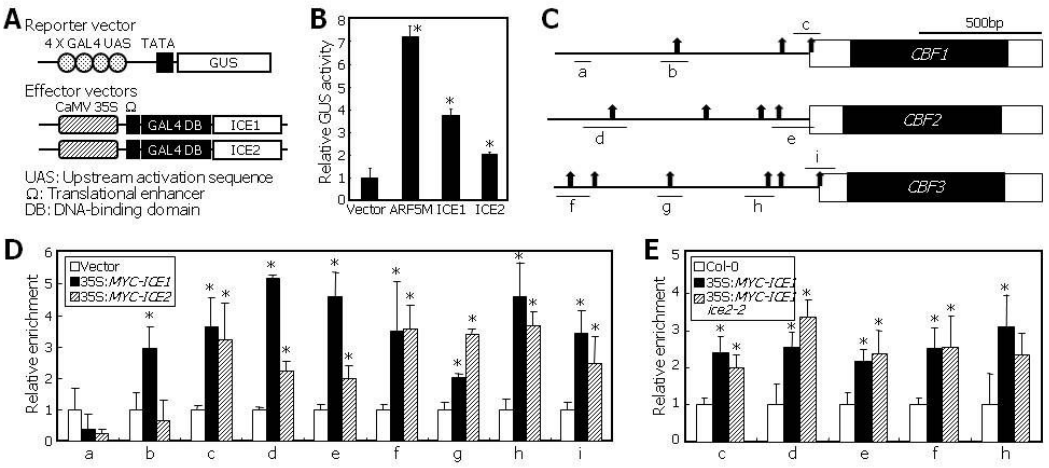

Figure 5. ICE1 and ICE2 Bind to *CBF* Promoters.

(A) Reporter and effector constructs used.

(B) Transcriptional activation activity assays of ICE1 and ICE2. The reporter and effector vectors were cotransformed into *Arabidopsis* protoplasts, and relative GUS activity was measured. ARF5M was used as activator control. Three measurements were averaged and statistically treated using Student *t*-test (**P*<0.01). Bars indicate SE.

(C) Potential MYC-recognition sequences in *CBF* promoters consisting of approximately 1.2-kbp sequences from the translation start sites. MYC-recognition sequences (CANNTG) are marked by bold arrows. The sequence regions a-h were used in ChIP assays. Black and white boxes indicate exons and untranslated regions, respectively. bp, base pair.

(D) ChIP assays on 35S:*MYC-ICE1* and 35S:*MYC-ICE2* transgenic plants. The 35S:*MYC-ICE* transgenic plants, in which a MYC-coding sequence was fused in-frame to the 5' ends of *ICE1*

and *ICE2* genes, were grown on MS-agar plates for 12 d. Plants were exposed to 4°C for 2.5 h, and ChIP assays were performed using an anti-MYC antibody. The level of immunoprecipitated DNA in vector control plants was set to 1. Four measurements were averaged and statistically treated (*t*-test, **P*<0.01). Bars indicate SE.

(E) ChIP assays on 35S:*MYC-ICE1 ice2-2* plants. ChIP assays were performed as described in **(D).**

ICE2 Overexpression Rescues the Freezing-Sensitive Phenotype of *ice1-2* Mutant

To obtain insights into the functional relationship between ICE1 and ICE2 in freezing tolerance, we examined the freezing tolerance of *ice1-2* mutant overexpressing *ICE2* driven by the CaMV 35S promoter (35S:*ICE2 ice1-2*). We found that *ICE2* overexpression efficiently rescued the low temperature-sensitive phenotype of the *ice1-2* mutant (Figure 6A), which was certainly attributable to the overexpression of *ICE2* by 6-fold (Figure 6B). Freezing tolerance assays showed that survival rate of the 35S:*ICE2 ice1-2* plants was higher than that of the *ice1-2* mutant and comparable to that of Col-0 plants (Figure 6C). Electrolyte leakage assays also supported the recovery of the freezing sensitivity of the *ice1-2* mutant by *ICE2* overexpression (Figure 6D). These observations, in combination with the increased freezing sensitivity of *ice1-2 ice2-2/+* plants, demonstrate that ICE1 and ICE2 function in an unequally redundant manner in the acquisition of freezing tolerance.

To find clues as to the molecular basis of the unequal functional redundancy between ICE1 and ICE2, we measured the transcript levels of *ICE1* or *ICE2* in Col-0 plants that were treated with cold temperature (4^{o}C). Cold temperature did not influence the transcription of the *ICE* genes (Figure 7A). We also examined the effects of cold temperature on the tissue-specific

expression patterns of *ICE2*. Transgenic plants expressing the *GUS* reporter gene driven by the endogenous *ICE2* promoter were exposed to 4°C. Histochemical GUS staining revealed that cold temperature did not alter the expression domains and levels of *ICE2* (Figure 7B). A distinction was observed between the expression domains of *ICE1* and *ICE2* genes in the root tissues. *ICE2* was expressed predominantly in the root tip and lateral root primordium (Figure 7C), unlike *ICE1* that is broadly expressed throughout the root tissues (Chinnusamy et al., 2003).

We next performed absolute quantitation of endogenous transcript levels of *ICE* genes. The results showed that the level of *ICE2* transcripts was approximately 60% of that of *ICE1* transcripts under both normal and cold conditions (Figure 7D). It is therefore likely that the unequal functional redundancy between ICE1 and ICE2 is derived from differential gene transcription.

Many homologous genes displaying unequal redundancy undergo cross regulation (Briggs et al., 2006). We therefore examined whether ICE1 regulate *ICE2* transcription and *vice versa*. The level of *ICE2* transcripts was reduced slightly but reproducibly in *ice1-2* mutant under both normal and cold temperature conditions (Figure 7E). Similarly, *ICE1* transcription was reduced to a similar degree in *ice2-2* mutant under identical conditions (Figure 7E). Together, these observations indicate that the unequal functional redundancy between ICE1 and ICE2 is modulated primarily at the transcriptional level through differential gene transcription

and cross regulation. The differential expression patterns of *ICE1* and *ICE2* genes in the root tissues may reflect functional diversification of the ICE proteins (see **DISCUSSION**).

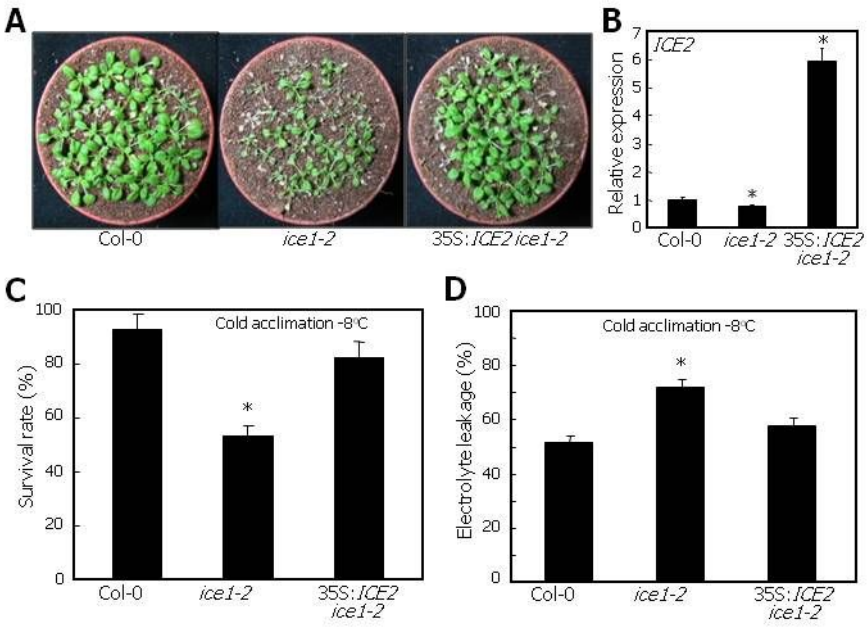

Figure 6. *ICE2* Overexpression Rescues *ice1-2* Phenotypes.

(A) Freezing tolerance of 35S:*ICE2 ice1-2* plants. *ICE2* gene was overexpressed driven by the CaMV 35S promoter in *ice1-2* mutant, resulting in 35S:*ICE2 ice1-2* plants. Twelve-day-old plant grown on MS-agar plates were transferred to soil and grown for 3 additional days. After cold acclimation at 4°C for 4 d, plants were exposed to -8°C for 3 h. After incubation at 4°C overnight for thawing, they were allowed to recover by incubating at 23°C for 7 d.

(B) Expression of *ICE2* in 35S:*ICE2 ice1-2* plants. Twelve-day-old plants grown on MS-agar plates were used for total RNA extraction. Relative mRNA levels were examined by qRT-PCR. Biological triplicates were averaged and statistically treated (*t*-test, **P*<0.01). Bars indicate SE.

(C and D) Survival tests **(C)** and electrolyte leakage assays **(D)** were performed as described in

Figure 2. Bars indicate SE.

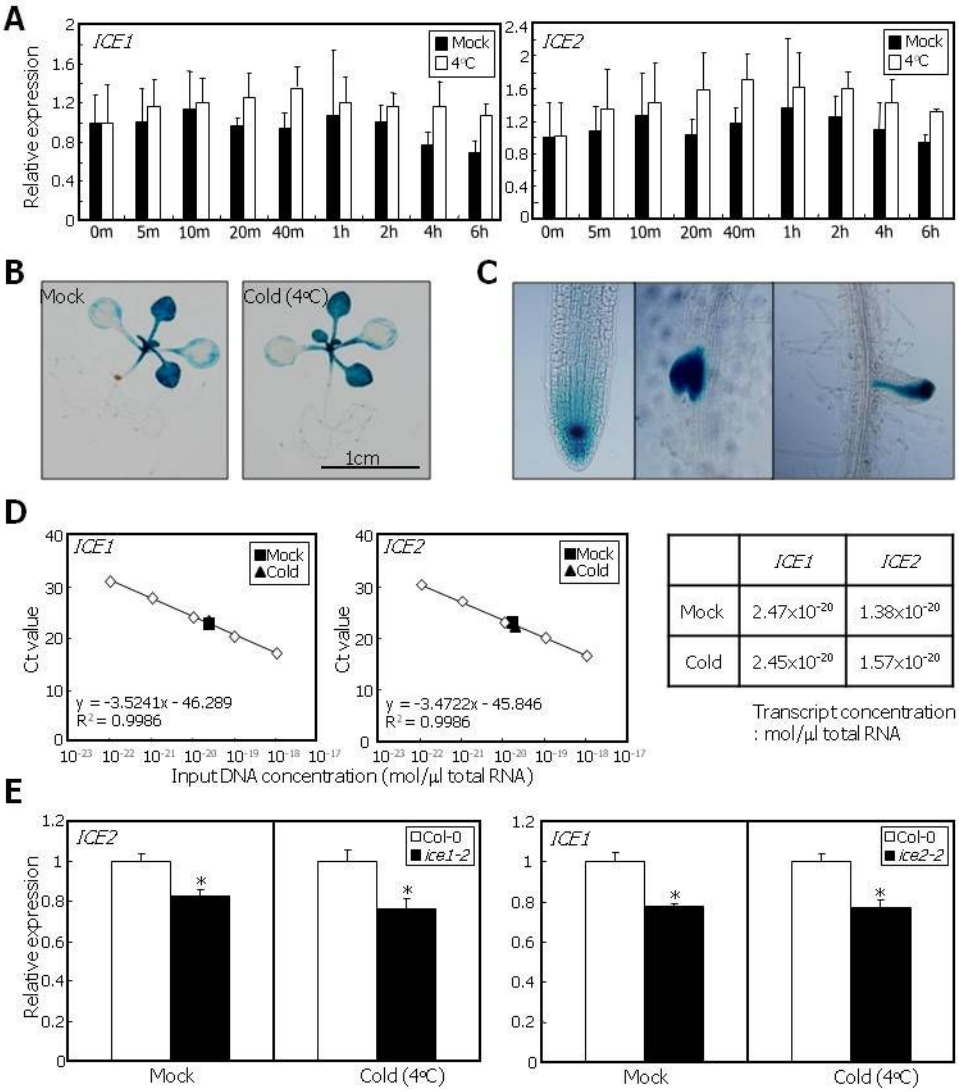

Figure 7. The Molecular Basis of the Unequal Functional Redundancy between ICE1 and ICE2. Twelve-day-old plants grown on MS-agar plates were used.

(A) Expression kinetics of *ICE* genes under cold conditions. Whole Col-0 plants were used for total RNA extraction. mRNA levels were examined by qRT-PCR. Biological triplicates were averaged and statistically treated using Student *t*-test (*$P<0.01$). Bars indicate SE.

(B) Expression pattern of *ICE2* gene. The promoter sequence of *ICE2* gene, consisting of approximately 4-kbp sequence upstream of the translational start site, was transcriptionally fused to the β-glucuronidase (GUS)-coding sequence, and the p*ICE2*:*GUS* reporter was transformed into Col-0 plants. The resultant transgenic seedling was exposed to 4°C for 1 h before histochemical GUS staining.

(C) *ICE2* expression in root tissue. The transgenic plant described in **(B)** was subjected to histochemical GUS staining and visualized by light microscopy.

(D) Absolute quantitation of *ICE1* and *ICE2* transcripts. Col-0 plants were exposed to 4°C for 1 h. Whole plants were used for total RNA extraction. The set of standards contains ten-fold serial dilutions of *ICE1* or *ICE2* transcripts. The regression line from the dilution curve was used to determine the concentrations of *ICE1* and *ICE2* transcripts.

(E) Cross regulation between *ICE1* and *ICE2* genes. *ice1-2* and *ice2-2* mutant plants were exposed to 4°C for 1 h. Whole plants were used for total RNA extraction. mRNA levels were examined by qRT-PCR. Biological triplicates were averaged and statistically treated using Student *t*-test (*$P<0.01$). Bars indicate SE.

ICE2 Is Ubiquitinated by HOS1

HOS1 is a cold-responsive E3 ubiquitin ligase that attenuates cold response by directing the degradation of ICE1 (Dong et al., 2006). On the basis of the redundant roles of ICE1 and ICE2, we assumed that ICE2 might also be targeted by HOS1.

To examine the physical interaction between ICE2 and HOS1, we generated a series of expression constructs encoding full-size and truncated forms of ICE2 and HOS1 proteins (Figure 8A). Yeast two-hybrid assays revealed that ICE2 and HOS1 interact with each other (Figure 8B). The interaction was mediated by the C-terminal domain of HOS1 and the C-terminal domain of ICE2 that harbors leucine zipper (ZIP) motif. The ICE2-HOS1 interaction was also verified by *in vitro* pull-down assays using recombinant maltose-binding protein (MBP)-HOS1 fusion protein produced in *Escherichia coli* cells and *in vitro* translated ICE2 polypeptides (Figure 8C). Bimolecular fluorescence complementation (BiFC) assays showed that the ICE2-HOS1 interaction occurs in the nucleus of plant cells (Figure 8D).

We next asked whether HOS1 degrades ICE2. The 35S:*MYC-ICE2* transgenic plants were treated with cold temperature (4^{o}C), and ICE2 proteins were immunologically detected using an anti-MYC antibody. ICE2 abundance declined rapidly 6 h after cold

exposure (Figure 8E). However, the cold-induced reduction of ICE2 abundance disappeared when the assays were performed in the presence of MG132 (Figure 8F), a potent inhibitor of 26S proteasome (Lee and Goldberg, 1998). In contrast, protease inhibitors did not affect the cold effects, indicating that ICE2 degradation occurs through the ubiquitin/proteasome-dependent pathway.

We suspected that the cold-induced degradation of ICE2 would be mediated by HOS1. The *MYC-ICE2* fusion was transformed into the *HOS1*-defective *hos1-3* mutant (Jung et al., 2012). The resultant transgenic plants were exposed to 4^{o}C, and ICE2 abundance was examined. As predicted, ICE2 degradation did not occur in the transgenic plants even under cold temperature conditions (Figure 8G), supporting that ICE2 degradation is mediated by HOS1.

We employed *in vivo* ubiquitination assays to confirm the HOS1-mediated degradation of ICE2. The *hos1-3* mutant overexpressing the *MYC-ICE2* fusion was exposed to 4^{o}C in the presence of MG132. ICE2 proteins were immunoprecipitated using an anti-MYC antibody, and ubiquitinated ICE2 proteins were immunologically detected using an anti-ubiquitin antibody. A ladder of ubiquitinated ICE2 proteins was detected in Col-0 background but largely disappeared in *hos1-3* background (Figure 8H), showing that HOS1-mediated ubiquitination of ICE2 occurs in plant cells.

Altogether, our data illustrate that ICE1 and ICE2 regulate the expression of *CBF* genes with unequal functional redundancy in inducing freezing tolerance, constituting a unified ICE-CBF cold acclimation pathway. They directly regulate *CBF1* and *CBF3* by binding to the gene promoters under low temperature conditions. Similarly, they also induce *CBF2* expression, whose gene product acts as a negative regulator of *CBF1* and *CBF3* (Novillo et al., 2004). Based on the previous and our own data, a plausible signaling scheme would be that the ICE-CBF2-CBF1/CBF3 module attenuates the CBF-mediated cold signaling at the transcriptional level (Figure 9). The feedback control of *CBF1* and *CBF3* by the ICE-CBF2 module would help sustain proper plant development and survival even under extended low temperature conditions.

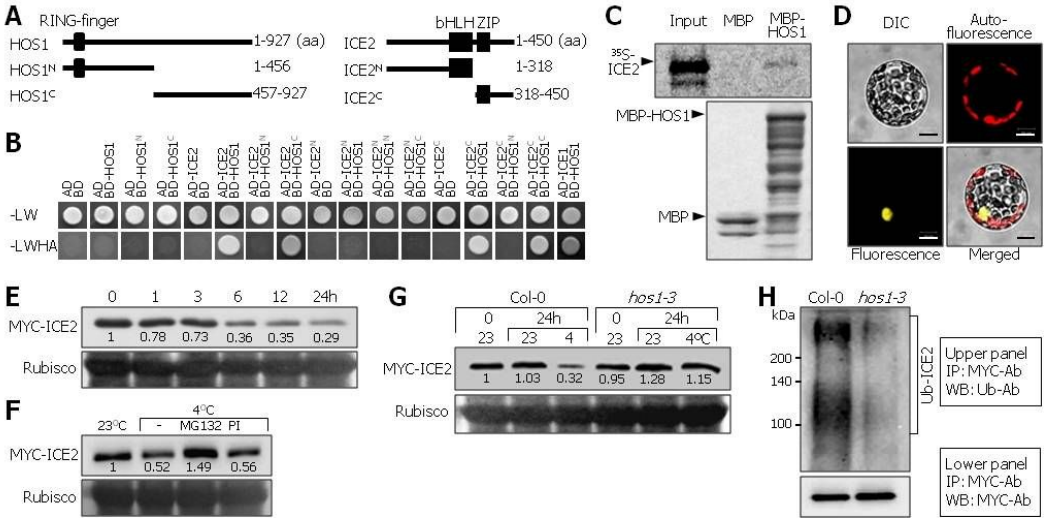

Figure 8. ICE2 Is Degraded by HOS1.

(A) ICE2 and HOS1 expression constructs used in yeast two-hybrid assays. aa, amino acid.

(B) ICE2-HOS1 interaction in yeast cells. The ICE2 and HOS1 cDNAs were fused to the GAL4 activation domain (AD)-coding sequence and GAL4 DNA-binding domain (BD) sequence, respectively. -LWHA represents Leu, Trp, His, and Ade dropout plates. -LW represents Leu and Trp dropout plates. Cell growth on -LWHA plates indicates positive interaction.

(C) *in vitro* pull-down assays. Recombinant MBP-HOS1 fusion proteins were produced in *E. coli* cells. ^{35}S-labeled ICE2 protein was prepared by *in vitro* translation (upper panel). Input represents 5% of the reaction. Recombinant MBP protein was used as negative control. Part of Coomassie blue-stained gel was shown as loading control (lower panel).

(D) BiFC assays. YFP^{N}-HOS1 and YFP^{C}-ICE2 fusions were transiently coexpressed in

Arabidopsis protoplasts. Protein interactions were visualized by differential interference contrast microscopy (DIC) and fluorescence microcopy. Scale bars = 10 μm.

(E) ICE2 abundance. Twelve-day-old 35S:*MYC-ICE2* transgenic plants grown on MS-agar plates were exposed to 4°C. Whole plants were used for the extraction of total proteins. ICE2 abundance was determined by Western blot analysis using an anti-MYC antibody (upper panel). Rubisco was used as loading control (lower panel). Numbers indicate relative ratios compared to that before cold treatment.

(F) Ubiquitin-mediated ICE2 degradation. Plants were exposed to 4°C, as described in **(E)**, in the presence of either MG132 or protease inhibitor (PI).

(G) ICE2 degradation in *hos1-3* mutant. The *MYC-ICE2* gene fusion was transformed driven by the CaMV 35S promoter into *hos1-3* mutant. Plants were exposed to 4°C, as described in **(E)**.

(H) *in vivo* ubiquitination assays. Plants described in **(E)** were grown on MS-agar plates for 8 d in the presence of 50 μM MG132 for 24 h and exposed to 4°C for 24 h. The MYC-ICE2 protein was immunoprecipitated using an anti-MYC antibody (IP). Ubiquitinated ICE2 protein was detected by Western blot analysis using an anti-ubiquitin antibody (WB). kDa, kilodalton.

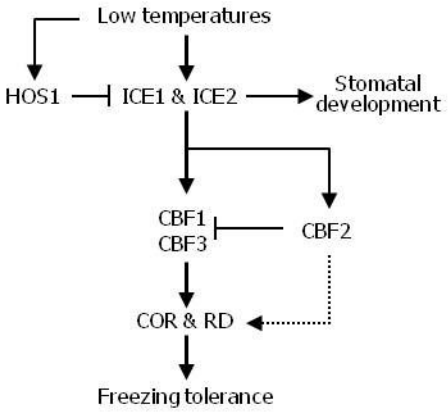

Figure 9. ICE-Mediated Transcriptional Feedback Loop Attenuates CBF Signaling.

Under low temperature conditions, ICE1 and ICE2 activate the expression of *CBF1*, *CBF2*, and *CBF3* by directly binding to the gene promoters. Note that *Arabidopsis* mutants that are defective in both *ICE1* and *ICE2* stop growing at seedling stages, suggesting that the combined function of ICE1 and ICE2 is important for plant development, such as stomatal differentiation (Kanaoka et al., 2008). The ICE-CBF2 signals suppress the expression of *CBF1* and *CBF3*, attenuating cold signaling.

DISCUSSION

ICE1 and ICE2 Are Master Regulators of CBF Signaling

Most recent studies on the role of ICE1 in freezing tolerance have been focused on the dominant negative *ice1-1* mutant (Chinnusamy et al., 2003). The *ice1-1* mutant exhibits reduced freezing tolerance, supporting that ICE1 function is disrupted in the mutant. However, the mutant displays an opposite phenotype to that of the T-DNA insertional *ice1-2* mutant in stomatal development (Kanaoka et al., 2008), obscuring the nature of the *ice1-1* mutation. ICE2 has also been suggested to play a role in plant responses to low temperature by regulating *CBF1* expression (Fursova et al., 2009). However, it was not fully understood at the molecular level whether and how ICE1 and ICE2 regulate the expression of *CBF1*, *CBF2*, and *CBF3*.

In this study, we employed multiple mutants that are defective in either *ICE1* or *ICE2* or both. We found that ICE1 and ICE2 act as master regulators of *CBF* expression. Both regulate the expression of *CBF1*, *CBF2*, and *CBF3* with unequal functional redundancy by directly binding to the gene promoters under low temperature conditions. Together with the overlapping roles of ICE1 and ICE2 in stomatal development (Kanaoka

et al., 2008), our data support that ICE1 and ICE2 mediate the physiological connection between stomatal development and cold acclimation. It will be worthy of examining stomatal differentiation in the single and double mutants that are defective in *ICE* genes under low temperature conditions.

ICE-CBF2 as An Attenuator of Cold Signaling

What is the physiological significance of the regulation of *CBF* genes by ICE1 and ICE2? It has been shown that CBF proteins are not functionally equivalent in the acquisition of freezing tolerance (Novillo et al., 2004, 2007). Low temperatures induce *CBF2* (Gilmour et al., 1998), which is directly regulated by ICE1 and ICE2 (this work). However, CBF2 negatively regulates the expression of *CBF1* and *CBF3* (Novillo et al., 2004).

Considering the induction of both *CBF2* and *CBF1*/*CBF3* by ICE1 and ICE2 under low temperature conditions, a most probable explanation would be that the ICE-CBF2 module acts as a cold signaling attenuator. Under prolonged low temperature conditions, *CBF1* and *CBF3* would be induced to very high levels, resulting in extreme cold response that would be harmful for sustained plant growth (Thomashow, 2010). It is therefore necessary that the ICE-CBF-COR regulon should be maintained at appropriate

levels so that plants can establish freezing tolerance while sustaining plant development. It is therefore concluded that the ICE-mediated transcriptional feedback loop modulates the ICE-CBF-COR regulon to balance the developmental and environmental adaptation processes.

There is a well-known precedent of cold-induced attenuation of cold signaling in plants. HOS1 E3 ubiquitin ligase, which is activated under low temperature conditions (Lee et al., 2001; Dong et al., 2006), directs the degradation of ICE1 and ICE2 via the ubiquitin/proteasome pathways (Dong et al., 2006, this work). It has been suggested that HOS1-mediated attenuation of cold signaling helps plants retain growth and development under low temperature conditions (Thomashow, 2010). Based on the previous and our own data, we propose that plant responses to low temperatures are finely tuned by the coordinated actions of the HOS1-mediated attenuation of ICE activity at the protein level and the CBF2-mediated attenuation of *CBF1* and *CBF3* expression at the transcription level (Figure 7).

Suppression of *CBF1* and *CBF3* by CBF2 would explain at least in part the weak phenotype of *ice1-2* mutant and no visible phenotype of *ice2-2* mutant at low temperatures. In the single mutants, the reduced induction of *CBF1* and *CBF3* would be compromised by the reduction of CBF2 activity through the ICE-CBF2 transcriptional

feedback loop.

Unequal Functional Redundancy between ICE1 and ICE2

Unequal genetic redundancy is frequently observed in homologous gene pairs that have evolved through gene duplication in plants (Briggs et al., 2006). It depicts that whereas mutations of ancestral gene have detectable phenotypes and those of duplicated gene show no visible phenotypes, double mutants usually exhibit severe phenotypes (Briggs et al., 2006).

There are two major causes of unequal functional redundancy: differential gene expression, which is more common, and cross regulation. Unequal functional redundancy between APETALLA 1 (AP1) and CAULIFLOWER (CAL) in floral development is probably caused by differential gene expression. It has been reported that the expression level of *AP1* gene is much higher than that of *CAL* gene (Kempin et al., 1995). Meanwhile, unequal functional redundancy between LONG HYPOCOTYL 5 (HY5) and HY5-HOMOLOG (HYH) in photomorphogenesis is derived from cross regulation (Holm et al., 2002).

On the basis of the differential freezing-sensitive phenotypes of *ice1-2* and *ice2-*

2 mutants and *ice1-2 ice2-2/+* plants and the higher level of endogenous *ICE1* transcripts than that of *ICE2* transcripts, we conclude that *ICE1* is an ancestral gene and *ICE2* is a duplicated gene. Cross regulation between ICE1 and ICE2 also contributes to the unequal functional redundancy between them.

Among the three evolutionary fates of homologous gene pairs, such as non-functionalization, sub-functionalization, and neo-functionalization, non-functionalization is most common in plants (Magadum et al., 2013). Partial complementation of the *ice1-2* phenotypes by *ICE2* overexpression suggests that *ICE2* is not in the process of non-functionalization. In support of this view, *ICE1* and *ICE2* are differentially expressed in the root tissues. It has been found that differential expression patterns of homologous gene pairs reflect either sub-functionalization or neo-functionalization (Duarte et al., 2006).

An additional cue supporting the evolutionary route of *ICE1* and *ICE2* is the presence of cathelicidin-like domain only in ICE2. Cathelicidin is an antimicrobial protein that protects host cells from microorganisms (Kosciuczuk et al., 2012). It has been reported that *ICE2*-overexpressing plants are resistant to bacterial infection (Tarasov et al., 2009). Although the dominant negative *ice1-1* mutant also exhibits enhanced disease resistance (Miura and Ohta, 2010; Zhu et al., 2011), it is unclear whether ICE1 has

antimicrobial activity or not. It will be worthy of examining whether ICE2 or ICE1 or both is involved in cold-induced pathogen resistance, as has been proven in some overwintering grasses (Kuwabara and Imai, 2009).

METHODS

Plant Materials and Growth Conditions

All *Arabidopsis thaliana* lines used were of the Columbia (Col-0) background, unless specified otherwise. The 35S:*ICE2 ice1-2* plants were produced by overexpressing *ICE2* driven by the CaMV 35S promoter in *ice1-2* mutant. To produce p*ICE1*:*ICE1 ice1-2* plants, *ICE1* was expressed under the control of the endogenous *ICE1* promoter consisting of approximately 4-kbp sequence upstream of the translational start site in *ice1-2* mutant. The 35S:*MYC-ICE2* transgenic plants were produced by transforming a *MYC-ICE2* fusion, in which a MYC-coding sequence was fused in-frame to the 5' end of *ICE2*, into Col-0 plants. *Agrobacterium tumefaciens*-mediated *Arabidopsis* transformation was conducted according to a modified floral dip method (Clough and Bent, 1998).

The *ice1-2* mutant (SALK-003155), which has been described previously (Kanaoka et al., 2008), was obtained from the *Arabidopsis* mutant pool of T-DNA insertional lines deposited in the *Arabidopsis* Biological Resource Center (ABRC, Ohio state University, Columbus, OH). The *ice2-2* mutant (GABI-Kat-175D04) was isolated

from the *Arabidopsis* mutant pool of T-DNA insertion lines deposited in the German Plant Genomics Research Program-Kölner *Arabidopsis* T-DNA lines (GABI-Kat) (Kleinboelting et al., 2012). The 35S:*MYC-ICE1* plants and *hos1-3* mutant have been described previously (Jung et al., 2012, 2013).

Arabidopsis seeds were cold-imbibed for 3 d at 4°C in complete darkness and allowed to germinate in a controlled culture room set at 23°C with relative humidity of 60%. They were grown under long days (LDs, 16-h light and 8-h dark) with white-light illumination (120 μmol photons m^{-2} s^{-1}) provided by FLR40D/A fluorescent tubes (Osram, Seoul, Korea).

Analysis of Transcript Levels

qRT-PCR was employed to determine gene transcript levels. Total RNA sample preparation, reverse transcription, and quantitative polymerase chain reaction were carried out according to the rules proposed by Udvardi et al. (2008) to ensure reproducible measurements.

qRT-PCR reactions were performed using 96-well blocks with an Applied Biosystems 7500 Real-Time PCR System (Foster City, CA) using the SYBR Green I

master mix in a volume of 20 μL. PCR primers used were listed in **Table 1**. The two-step thermal cycling profile used was 15 s at 95°C and 1 min at 60°C. An *eIF4A* gene (At3g13920) was included in the PCR reactions as internal control in order to normalize the variations in the amounts of cDNA used.

qRT-PCR reactions were performed in biological triplicates using RNA samples extracted from three independent plant materials grown under identical conditions. The comparative $\Delta\Delta C_T$ method was employed to evaluate relative quantities of each product amplified from the samples. The threshold cycle (C_T) was automatically determined for each reaction by using the default parameters of the system.

Absolute Quantitation of Gene Transcripts

For absolute quantification of endogenous *ICE1* and *ICE2* transcripts, the cDNAs of *ICE1* and *ICE2* were subcloned into the pGADT7 vector (Clontech, Mountain View, CA) through homologous recombination of the EcoRI and BamH1 sites. An absolute standard curve of each transcript was generated by 10-fold serial dilutions ranging from 10^{-18} to 10^{-22} mol, as described previously (Whelan et al., 2003). Col-0 plants grown on MS-agar plates for 12 d were exposed to 4°C for 1 h. Whole plants were harvested for the

extraction of total RNA. Quantitative RT-PCR was performed using the SYBR Green I master mix (Applied Biosystems) with gene-specific primers listed in **Table 1.**

Primers	Sequences	Usage
eIF4A-F	5'-TGACCACACAGTCTCTGCAA	qRT-RCR
eIF4A-R	5'-ACCAGGGAGACTTGTTGGAC	qRT-RCR
CBF1-F	5'-GCATGTCTCAACTTCGCTGA	qRT-RCR
CBF1-R	5'-ATCGTCTCCTCCATGTCCAG	qRT-RCR
CBF2-F	5'-TGACGTGTCCTTATGGAGCTA	qRT-RCR
CBF2-R	5'-CTGCACTCAAAAACATTTGCA	qRT-RCR
CBF3-F	5'-GATGACGACGTATCGTTATGGA	qRT-RCR
CBF3-R	5'-TACACTCGTTTCTCAGTTTTACAAAC	qRT-RCR
COR15A-F	5'-GCAGATGGTGAGAAAGCGAA	qRT-RCR
COR15A-R	5'-GGCATCCTTAGCCTCTCCTG	qRT-RCR
RD29A-F	5'-GTTACTGATCCCACCAAAGAAGA	qRT-RCR
RD29A-R	5'-GGAGACTCATCAGTCACTTCCA	qRT-RCR
KIN1-F	5'-TGGAGCTGGAGCACAACA	qRT-RCR
KIN1-R	5'-GACCCGAATCGCTACTTGTTC	qRT-RCR
COR47-F	5'-GGACACCACGACAAGACAGC	qRT-RCR
COR47-R	5'-CGTGACAGCTGGTGAATCCT	qRT-RCR
MYB15-F	5'-GGTGCGGATATCGATGAAAG	qRT-RCR
MYB15-R	5'-CATTATTAGCGGAGCCCAAG	qRT-RCR
ICE1-F	5'-AATTGGGGAACAGGGATTTG	qRT-RCR
ICE1-R	5'-CAACGGAGCTGTGAAACCAC	qRT-RCR
ICE2-F	5'-TCTTCAAGCTTGCATCCGTT	qRT-RCR
ICE2-R	5'-GTTGGCCTTTAGGACTTGGC	qRT-RCR

Table 1. Primers Used.

Yeast Two-Hybrid Assay

Yeast two-hybrid assays were performed using the BD Matchmaker system (Clontech). The pGADT7 vector was used for GAL4 AD (activation domain), and the pGBKT7 vector was used for GAL4 BD (DNA-binding domain). Yeast strain AH109 (leu-, trp-, ade-, his-), which has the chromosomally integrated reporter genes *lacZ* and *HIS* under

the control of the GAL1 promoter, was used for transformation. The PCR products of *ICE2* were digested with EcoRI and BamHI for subcloning into the pGADT7 vector. The *HOS1* constructs in the pGBKT7 vector have been described previously (Jung et al., 2012). Transformation of AH109 cells was performed according to the manufacturer's instruction.

in vitro Pull-Down Assay

Recombinant MBP and MBP-HOS1 fusion proteins were produced in *E. coli* Rosetta2 (DE3) pLysS strain (Novagen, Madison, WI) and partially purified, as described previously (Jung et al., 2012).

The *ICE2* cDNA was subcloned into the pGADT7 vector. The ICE2 polypeptides were labeled with ^{35}S-Met by *in vitro* translation using the TNT coupled reticulocyte lysate system (Promega, Madison, WI).

Amylose resin (Sigma-Aldrich) and binding buffer (50 mM Tris-Cl, pH 8.0, 100 mM NaCl, 10% glycerol, 1% Triton X-100, 1 mM PMSF) containing protease inhibitor cocktail were agitated with ^{35}S-labeled ICE2 and HOS1 proteins for 12 h at 4^{o}C. Beads were washed 10 times with TN buffer (25 mM Tris-Cl, pH 8.0, 100 mM NaCl). The

bound proteins were eluted with 2X SDS-PAGE loading buffer by boiling for 5 min and subject to SDS-PAGE and autoradiography.

BiFC

BiFC assays were performed by cotransfection of YFP^N-HOS1 and YFP^C-ICE2 vectors into *Arabidopsis* mesophyll protoplasts by a polyethylene glycol (PEG)-calcium transfection method (Yoo et al., 2007). The subcellular distribution of HOS-ICE2 interactions was visualized by differential interference contrast microscopy (DIC) and fluorescence microscopy. Reconstitution of YFP fluorescence was observed using the Zeiss LSM510 confocal microscope (Carl Zeiss, Jena, Germany) with the following YFP filter setup: excitation 515 nm, 458/514 dichroic, and emission 560-615 nm BP filter.

Transcriptional Activation Activity Assay

For transient expression assays in *Arabidopsis* protoplasts, a series of reporter and effector plasmids was constructed. The reporter plasmids contain 4 copies of the GAL4 upstream activation sequence fused to a TATA sequence and *GUS* gene. To construct the

p35S:*ICE* effector plasmids, the *ICE1* or *ICE2* cDNA was fused to the GAL4 BD-coding sequence, and the fusion was inserted into an expression vector containing the CaMV 35S promoter. The reporter and effector plasmids were cotransformed into *Arabidopsis* protoplasts by a PEG-mediated transformation method. GUS activity was measured by the fluorometric method, as described previously (Jefferson et al., 1987). A CaMV 35S promoter-luciferase construct was also cotransformed as internal control. The luciferase assay was performed using the Luciferase Assay System kit (Promega).

ChIP

An MYC-coding sequence was fused in-frame to the 5' ends of *ICE1* and *ICE2* cDNAs, and the fusions were subcloned under the control of the CaMV 35S promoter. The expression construct was transformed into Col-0 plants, resulting in 35S:*MYC-ICE1* and 35S:*MYC-ICE2* transgenic plants. Twelve-day-old 35S:*MYC-ICE* transgenic plants grown on MS-agar plates were incubated at 4°C for 2.5 h and used for the extraction of total cellular extracts. ChIP assays were performed as described previously (Gendrel et al., 2005). An anti-MYC antibody was used for immunoprecipitation. DNA was purified using the Wizard SV Gel and PCR Clean-Up system (Promega).

Freezing Tolerance Assay

Approximately 25-30 plants grown for 12 d on MS-agar plates under LDs were transferred to soil and grown for 3 additional days. They were treated at 0°C for 30 min before freezing temperature treatments. Temperature was set to -1°C/30 min decrease. The plants were then incubated for 3 h at desired freezing temperatures. Temperature was restored to 4°C by 1°C increase per 30 min. The plants were incubated at 4°C in the dark overnight for thawing and allowed to recover by incubating at 23°C for 7 d.

Electrolyte Leakage Assay

Freezing treatments were performed as described above. After thawing at 4°C in the dark overnight, aerial plant parts were soaked in 20 mL of deionized water. The plant samples were agitated overnight, and conductivity of the water was measured using Orion 5-star conductivity meter (Thermo, Beverly, MA). The tubes containing the plant materials were then autoclaved at 120°C for 10 min. After cooling to room temperature, conductivity was measured (100% conductivity), and percentage of electrolyte leakage was calculated.

Histochemical Staining

Approximately 4-kb promoter sequences upstream of the translational start sites of *ICE1* and *ICE2* genes were transcriptionally fused to the 5' ends of *GUS* sequence, and the fusion constructs were transformed into Col-0 plants. Histochemical staining of GUS activity was conducted as described previously (Jung et al., 2012). The plant samples were then mounted on microscope slide glasses and visualized using a DIMIS-M digital camera (JMTECH, Seoul, Korea).

ICE2 Degradation Assay

The 35S:*MYC-ICE2* transgenic plants grown on MS-agar plates for 12 d were exposed to 4°C for appropriate time periods. To examine the effects of MG132 and protease inhibitor on ICE2 protein stability, the 35S:*MYC-ICE2* transgenic plants were incubated in MS liquid media containing either 50 μM MG132 or protease inhibitor cocktail (Sigma-Aldrich) at 4°C for 5 h. To examine the effects of *hos1* mutation, the *MYC-ICE2* gene fusion was transformed driven by the CaMV 35S promoter into *hos1-3* mutant, and the resultant 35S:*MYC-ICE2 hos1-3* plants were subject to cold treatment as described

above. Whole plants were used for the preparation of protein extracts. ICE2 proteins were detected by Western blot analysis using an anti-MYC antibody. The band intensities on the Western blots were quantitated using the ImageJ software (http://rsbweb.nih.gov/ij/), as described previously (Wardle et al., 2011).

in vivo Ubiquitination Assay

in vivo ubiquitination of ICE2 was assayed as described previously (Jung et al., 2012) with some modifications. Eight-day-old transgenic plants overexpressing *ICE2* gene in Col-0 and *hos1-3* backgrounds were pretreated with 50 μM MG132 for 24 h and then incubated at 4°C for additional 24 h. Isolation of nuclei from the *ICE2*-overexpressing plants and preparation of nuclear extract were performed as described previously (Gendrel et al. 2005). Nuclear extracts were immunoprecipitated using an anti-MYC antibodies conjugated to protein A-agarose beads for 3 h at 4°C. Beads were then washed 5 times, and bound proteins were eluted with 2X SDS loading buffer by boiling for 5 min. The eluted protein was analyzed immunologically using anti-ubiquitin and anti-MYC antibodies.

Statistical Analysis

The statistical significance between two means of measurements were determined using Student *t*-test with P values<0.01.

REFERENCES

Agarwal, M., Hao, Y., Kapoor, A., Dong, C.H., Fujii, H., Zheng, X., and Zhu, J.K. (2006). A R2R3 type MYB transcription factor is involved in the cold regulation of *CBF* genes and in acquired freezing tolerance. J. Biol. Chem. **281:** 37636–37645.

Akhtar, M., Jaiswal, A., Taj, G., Jaiswal, J.P., Qureshi, M.I., and Singh, N.K. (2012). DREB1/CBF transcription factors: their structure, function and role in abiotic stress tolerance in plants. J. Genet. **91:** 385–395.

Briggs, G.C., Osmont, K.S., Shindo, C., Sibout, R., and Hardtke, C.S. (2006). Unequal genetic redundancies in *Arabidopsis* – a neglected phenomenon? Trends Plant Sci. **11:** 492-498.

Chinnusamy, V., Ohta, M., Kanrar, S., Lee, B.H., Hong, X., Agarwal, M., and Zhu, J.K. (2003). ICE1: a regulator of cold-induced transcriptome and freezing tolerance in *Arabidopsis*. Genes Dev. **17:** 1043–1054.

Chinnusamy, V., Zhu, J., and Zhu, J.K. (2007). Cold stress regulation of gene expression in plants. Trends Plant Sci. **12:** 444–451.

Clough, S.J., and Bent, A.F. (1998). Floral dip: A simplified method for *Agrobacterium*-mediated transformation of *Arabidopsis thaliana*. Plant J. **16:** 735–743.

Doherty, C.J., Van Buskirk, H.A., Myers, S.J., and Thomashow, M.F. (2009). Roles for *Arabidopsis* CAMTA transcription factors in cold-regulated gene expression and freezing tolerance. Plant Cell **21:** 972–984.

Dong, C.H., Agarwal, M., Zhang, Y., Xie, Q., and Zhu, J.K. (2006). The negative regulator of plant cold responses, HOS1, is a RING E3 ligase that mediates the ubiquitination and degradation of ICE1. Proc. Natl Acad. Sci. USA **103:** 8281–8286.

Duarte, J.M., Cui, L., Wall, P.K., Zhang, Q., Zhang, X., Leebens-Mack, J., Ma, H., Altman, N., and dePamphilis, C.W. (2006). Expression pattern shifts following duplication indicative of subfunctionalization and neofunctionalization in regulatory genes of *Arabidopsis*. Mol. Biol. Evol. **23:** 469–478.

Fursova, O.V., Pogorelko, G.V., and Tarasov, V.A. (2009). Identification of *ICE2*, a gene involved in cold acclimation which determines freezing tolerance in *Arabidopsis thaliana*. Gene **429:** 98–103.

Gendrel, A.V., Lippman, Z., Martienssen, R., and Colot, V. (2005). Profiling histone modification patterns in plants using genomic tiling microarrays. Nat. Methods **2:** 213–218.

Gilmour, S.J., Fowler, S.G., and Thomashow, M.F. (2004). *Arabidopsis* transcriptional activators CBF1, CBF2, and CBF3 have matching functional activities. Plant Mol. Biol. **54:** 767–781.

Gilmour, S.J., Sebolt, A.M., Salazar, M.P., Everard, J.D., and Thomashow, M.F. (2000). Overexpression of the *Arabidopsis* CBF3 transcriptional activator mimics multiple biochemical changes associated with cold acclimation. Plant Physiol. **124:** 1854–1865.

Gilmour, S.J., Zarka, D.G., Stockinger, E.J., Salazar, M.P., Houghton, J.M., and Thomashow, M.F. (1998). Low temperature regulation of the *Arabidopsis* CBF family of AP2 transcriptional activators as an early step in cold-induced *COR* gene expression. Plant J. **16:** 433–442.

Guy, C., Kaplan, F., Kopka, J., Selbig, J., and Hincha, D.K. (2008). Metabolomics of temperature stress. Physiol. Plant. **132:** 220−235.

Hofmann, N.R. (2008). They all scream for ICE1/SCRM2: Core regulatory units in stomatal development. Plant Cell **20:** 1732

Holm, M., Ma, L.G., Qu, L.J., and Deng, X.W. (2002). Two interacting bZIP proteins are direct targets of COP1-mediated control of light dependent gene expression in *Arabidopsis*. Genes Dev. **16:** 1247-1259.

Jefferson, R.A., Kavanagh, T.A., and Bevan, M.W. (1987). GUS fusions: Beta-glucuronidase as a sensitive and versatile gene fusion marker in higher plants. EMBO J. **6:** 3901–3907.

Jung, J.H., Park, J.H., Lee, S., To, T.K., Kim, J.M., Seki, M., and Park, C.M. (2013). The cold signaling attenuator HIGH EXPRESSION OF OSMOTICALLY RESPONSIVE GENE1 activates *FLOWERING LOCUS C* transcription via chromatin remodeling under short-term cold stress in *Arabidopsis*. Plant Cell **25:** 4378-4390.

Jung, J.H., Seo, P.J., and Park, C.M. (2012). The E3 ubiquitin ligase HOS1 regulates *Arabidopsis* flowering by mediating CONSTANS degradation under cold stress. J. Biol. Chem. **287:** 43277–43287.

Kanaoka, M.M., Pillittere, L.J., Fujii, H., Yoshida, Y., Bogenschutz, N.L., Takabayashi, J., Zhu, J.K., and Torii, K.U. (2008). SCREAM/ICE1 and SCREAM2 specify three cell-state transitional steps leading to *Arabidopsis* stomatal differentiation. Plant Cell **20:** 1775–1785.

Kempin, S.A., Savidge, B., and Yanofsky, M.F. (1995). Molecular basis of the *cauliflower* phenotype in *Arabidopsis*. Science **267:** 522-525.

Kleinboelting, N., Huep, G., Kloetgen, A., Viehoever, P., and Weisshaar, B. (2012). GABI-Kat SimpleSearch: new features of the *Arabidopsis thaliana* T-DNA mutant database. Nucleic Acids Res. **40:** D1211–D1215.

Kosciuczuk, E.M., Lisowski, P., Jarczak, J., Strzalkowska, N., Jozwik, A., Horbanczuk, J., Krzyzewski, J., Zwierzchowski, L., and Bagnicka, E. (2012). Cathelicidins: Family of antimicrobial peptides. A review. Mol. Biol. Rep. **39:** 10957–10970.

Kuwabara, C., and Imai, R. (2009). Molecular basis of disease resistance acquired through cold acclimation in overwintering plants. J. Plant Biol. **52:** 19–26.

Lee, D.H., and Goldberg, A.L. (1998). Proteasome inhibitors: valuable new tools for cell biologists. Trends Cell Biol. **8:** 397–403.

Lee, C.M., and Thomashow, M.F. (2012). Photoperiodic regulation of the C-repeat binding factor (CBF) cold acclimation pathway and freezing tolerance in *Arabidopsis thaliana*. Proc. Natl. Acad. Sci. USA **109:** 15054–15059.

Lee, H., Xiong, L., Gong, Z., Ishitani, M., Stevenson, B. and Zhu, J.K. (2001). The *Arabidopsis* HOS1 gene negatively regulates cold signal transduction and encodes a RING finger protein that displays cold-regulated nucleo–cytoplasmic partitioning. Genes Dev. **15:** 912-924.

Magadum, S., Banerjee, U., Murugan, P., Gangapur, D., and Ravikesavan, R. (2013). Gene duplication as a major force in evolution. J. Genet. **92:** 155–161.

Matsui, A., Ishida, J., Morosawa, T., Mochizuki, Y., Kaminuma, E., Endo, T.A., Okamoto, M., Nambara, E., Nakajima, M., Kawashima, M., Satou, M., Kim, J.M., Kobayashi, N., Toyoda, T., Shinozaki, K., and Seki, M. (2008). *Arabidopsis* transcriptome analysis under drought, cold, high-salinity and ABA treatment conditions using a tiling array. Plant Cell Physiol. **49:** 1135–1149.

Medina, J., Catalá, R., and Salinas, J. (2011). The CBFs: Three *Arabidopsis* transcription factors to cold acclimate. Plant Sci. **180:** 3–11.

Meshi, T., and Iwabuchi, M. (1995). Plant transcription factors. Plant Cell Physiol. **36:** 1405−1420.

Miura, K., Jin, J.B., Lee, J., Yoo, C.Y., Stirm, V., Miura, T., Ashworth, E.N., Bressan, R.A., Yun, D.J., and Hasegawa, P.M. (2007). SIZ1-mediated sumoylation of ICE1 controls *CBF3/DREB1A* expression and freezing tolerance in *Arabidopsis*. Plant Cell **19:** 1403–1414.

Miura, K., and Ohta, M. (2010). SIZ1, a small ubiquitin-related modifier ligase, controls cold signaling through regulation of salicylic acid accumulation. J Plant Physiol. **167:** 555-560.

Novillo, F., Alonso, J.M., Ecker, J.R., and Salinas, J. (2004). CBF2/DREB1C is a negative regulator of *CBF1/DREB1B* and *CBF3/DREB1A* expression and plays a central role in stress tolerance in *Arabidopsis*. Proc. Natl Acad. Sci. USA **101:** 3985–3990.

Novillo, F., Medina, J., and Salinas, J. (2007). *Arabidopsis* CBF1 and CBF3 have a different function than CBF2 in cold acclimation and define different gene classes in the CBF regulon. Proc. Natl Acad. Sci. USA **104:** 21002–21007.

Sakuma, Y., Liu, Q., Dubouzet, J.G., Abe, H., Shinozaki, K. and Yamaguchi-Shinozaki, K. (2002). DNA-binding specificity of the ERF/AP2 domain of Arabidopsis DREBs, transcription factors involved in dehydration and cold-inducible gene expression. Biochem. Biophys. Res. Commun. **290:** 998–1009.

Tarasov, V.A., Khadeeva, N.V., Mel'nik, V.A., Ezhova, T.A., and Shestakov, S.V. (2009). The atlg12860 gene of *Arabidopsis thaliana* determines cathelicidin-like antimicrobial activity. Dokl. Biol. Sci. **427:** 332–334.

Thomashow, M.F. (2010). Molecular basis of plant cold acclimation: insights gained from studying the CBF cold response pathway. Plant Physiology **154:** 571–577.

Udvardi, M.K., Czechowski, T., and Scheible, W.R. (2008). Eleven golden rules of quantitative RT-PCR. Plant Cell **20:** 1736–1737.

Wardle, D.J., Burgon, J., Sabroe, I., Bingle, C.D., Whyte, M.K., and Renshaw., S.A. (2011). Effective caspase inhibition blocks neutrophil apoptosis and reveals Mcl-1 as both a regulator and a target of neutrophil caspase activation. PLoS One **6:** e15768.

Whelan, J.A., Russell, N.B., and Whelan, M.A. (2003). A method for the absolute quantification of cDNA using real-time PCR. J. Immunol. Methods **278:** 261–269.

Yoo, S. D., Cho, Y. H., and Sheen, J. (2007). *Arabidopsis* mesophyll protoplasts. A versatile cell system for transient gene expression analysis. Nat. Protoc. **2:** 1565−1572.

Zeller, G., Henz, S.R., Widmer, C.K., Sachsenberg, T., Rätsch, G., Weigel, D., and Laubinger, S. (2009). Stress-induced changes in the *Arabidopsis thaliana* transcriptome analyzed using whole-genome tiling arrays. Plant J. **58:** 1068–1082.

Zhu, Y., Yang, H., Mang, H.G., and Hua, J. (2011). Induction of *BAP1* by a moderate decrease in temperature is mediated by ICE1 in *Arabidopsis*. Plant Physiol. **155:** 580–588.

국문초록

CBF는 하위의 *COR* 유전자 발현을 활성화시킴으로써 애기장대의 저온순화과정을 유도하는 대표적인 전사인자다. CBF의 조절 인자로는 ICE1이 가장 잘 알려져 있지만, 그 중요성에 비해 ICE1의 *CBF* 유전자에 대한 조절 기작은 정확히 밝혀지지 않았다. 본 연구에서는 ICE1과 그 homolog인 ICE2가 *CBF1*, *CBF2*, *CBF3*의 promoter에 있는 MYC-recognition sequence에 결합하여 저온 특이적 발현을 유도한다는 것을 밝혔다. 또한, ICE1과 마찬가지로 ICE2 역시 저온에서 HOS1이라는 E3 ubiquitin 연결효소에 의해 단백질 수준에서 조절 받는다는 것을 확인하였다. 더 나아가, 저온 특이적인 표현형이 *ice1*, *ice2* 단일 돌연변이체보다 두 돌연변이체의 교배체에서 더욱 심화되는 것으로 보아 homolog인 두 ICE 단백질이 저온에서 redundant하게 작용한다는 것을 알 수 있었다. 본 연구결과와 CBF2가 *CBF1*, *CBF3*를 음성 조절한다는 기존 보고를 토대로, 본 실험실에서는 ICE-CBF 신호전달경로가 저온순화과정에서 CBF가 일시적으로 발현되도록 조절함으로써 식물의 성장 및 발달과 freezing tolerance 사이의 균형을 유지할 수 있게 해주는 되먹임 회로를 제공할 것임을 주장하고자 한다.

주요어: ICE, CBF, 저온순화과정, 되먹임 회로, Unequal redundancy, 애기장대

학번: 2012-20270